The Journal of Experimental Biology **198**, 1021–1027 (1995)
Printed in Great Britain © The Company of Biologists Limited 1995

THE FORCE–VELOCITY RELATIONSHIP OF THE ATP-DEPENDENT ACTIN–MYOSIN SLIDING CAUSING CYTOPLASMIC STREAMING IN ALGAL CELLS, STUDIED USING A CENTRIFUGE MICROSCOPE

S. CHAEN, J. INOUE AND H. SUGI*

Department of Physiology, School of Medicine, Teikyo University, Itabashi-ku, Tokyo 173, Japan

Accepted 15 November 1994

Summary

When uncoated polystyrene beads suspended in Mg-ATP solution were introduced into the internodal cell of an alga *Chara corallina*, the beads moved along the actin cables with directions and velocities (30–62 $\mu m\,s^{-1}$) similar to those of native cytoplasmic streaming. Bead movement was inhibited both in the absence of ATP and in the presence of Ca^{2+}, as with native cytoplasmic streaming. These results indicate that bead movement is caused by cytoplasmic myosin molecules attached to the bead surface interacting with actin cables. The steady-state force–velocity relationship of the actin–myosin sliding that produces cytoplasmic streaming was determined by applying constant centrifugal forces to the beads moving on the actin cables. The force–velocity curve in the positive load region was nearly straight, and the implications of this shape are discussed in connection with the kinetic properties of the actin–myosin interaction in cytoplasmic streaming. It is suggested that the time for which a cytoplasmic myosin head is detached from actin in one cycle of actin–myosin interaction is very short. The Ca^{2+}-induced actin–myosin linkages, responsible for the Ca^{2+}-induced stoppage of cytoplasmic streaming, were shown to be much stronger than the rigor actin–myosin linkages.

Key words: force–velocity relationship, cytoplasmic streaming, alga, actin–myosin sliding, *Chara corallina*.

Introduction

Although evidence has been accumulating that ATP-dependent actin–myosin interaction is responsible not only for muscle contraction but also for various types of non-muscle cell motility, including cytoplasmic streaming (Shimmen, 1992), no information is available about the kinetic properties of the actin–myosin interactions occurring in non-muscle cells. Green algae consist of giant internodal cells, in which cytoplasmic streaming is caused by sliding between actin filament arrays (actin cables) and myosin molecules in the cytoplasm (Kamiya and Kuroda, 1956; Nagai and Rebhum, 1966; Kersey and Wessels, 1976; Kato and Tonomura, 1977). The velocity of cytoplasmic streaming (50 $\mu m\,s^{-1}$ or more; Shimmen, 1992) is very rapid, being many times larger than the maximum velocity of myofilament sliding in muscle (5–10 $\mu m\,s^{-1}$). Algal internodal cells have been widely used for *in vitro* assays of myosin-based motility, since latex beads coated with skeletal, cardiac and smooth muscle myosins slide on the actin cables in an ATP-dependent manner in these cells. Unfortunately, however, it has not been possible to produce sliding between algal cell cytoplasmic myosin and the actin cables responsible for native cytoplasmic streaming.

Recently, we found that if uncoated polystyrene beads suspended in Mg-ATP solution were simply introduced into the interior of the internodal cell, the beads moved along the actin cables as a result of the attachment of cytoplasmic myosin molecules to the bead surface; both the velocity and the direction of the bead movement were similar to those of native cytoplasmic streaming. We could therefore determine the steady-state force–velocity relationship of the ATP-dependent actin–myosin sliding responsible for cytoplasmic streaming, using a centrifuge microscope with which constant centrifugal forces were applied to the moving beads to serve as external loads (Oiwa *et al.* 1990). It will be shown in the present paper that the force–velocity curve in the positive load region is nearly straight in shape, with a large value of a/P_0, where a is a constant from the Hill equation and P_0 is maximum isometric force, suggesting a high cycling rate and a low efficiency of the actin–myosin interaction in cytoplasmic streaming. Since cytoplasmic streaming is known to be inhibited by Ca^{2+} as well as by removal of ATP (Williamson, 1975; Tominaga *et al.* 1983), we also studied the behaviour of the beads in the absence of ATP and in the presence of Ca^{2+}.

*Author for correspondence.

Materials and methods

Internodal cell preparation

The green alga *Chara corallina* was cultured using the method of Shimmen and Yano (1984). Before experiments, the internodal cells (diameter approximately 0.5 mm; length 10–15 cm) were isolated from neighbouring cells and stored in artificial pond water containing 0.1 mmol l^{-1} each of KCl, NaCl and $CaCl_2$ (pH 5.6). The velocity of native cytoplasmic streaming was measured using the method of Kamiya and Kuroda (1956), and cells that exhibited prominent cytoplasmic streaming at a velocity of 30–60 μm s^{-1} were chosen for the experiments. The cell was cut open at both ends, and its cytoplasm and cell sap were replaced with Mg-ATP solution containing 5 mmol l^{-1} EGTA, 6 mmol l^{-1} $MgCl_2$, 1 mmol l^{-1} ATP, 200 mmol l^{-1} sorbitol, 50 mmol l^{-1} KOH and 20 mmol l^{-1} Pipes (pH 7.0) by perfusion of the cell interior with several times the cell volume of Mg-ATP solution (Tazawa *et al.* 1976).

Tosyl-activated polystyrene beads (Dynabeads, Dynal, Oslo; diameter 2.8 μm; specific gravity 1.3) were suspended in Mg-ATP solution (10^7 beads ml^{-1}) without previous coating procedures and introduced into the cell at a late stage of the perfusion. As described below, the beads moved along the actin cables as a result of spontaneous attachment to cytoplasmic myosin molecules remaining in the cell interior. Both ends of the cell containing the polystyrene beads were ligated with strips of polyester thread (Oiwa *et al.* 1990). The internodal cell preparations (approximately 1 cm in length) were kept in artificial pond water.

Centrifuge microscope and video recording system

The centrifuge microscope consisted of a light microscope, a rotor (diameter 16 cm) that could be rotated at 250–5000 revs min^{-1} (4–1900 ***g***), and a stroboscopic light source to allow a stationary image of the specimen to be observed during centrifugation. A video-enhanced-contrast image of the specimen was obtained with a video camera (Hamamatsu Photonics, C-2847) combined with circuits for real-time differential treatment of the image signal. The video image was recorded with a video casette recorder (Sony, VO-9600) at 30 frames s^{-1}. Further details of the centrifuge microscope and the video recording system have been described elsewhere (Kamitsubo *et al.* 1989; Oiwa *et al.* 1990).

Experimental procedures

The internodal cell preparation containing the polystyrene beads was placed in a centrifuge cuvette (33 mm× 24 mm×3 mm deep), filled with artificial pond water, and mounted on the rotor of the centrifuge microscope so that its chloroplast rows, along which the actin cables extend in a straight line, were parallel to the direction of centrifugal force. Bead movement along the actin cables was observed and video-recorded with a Nikon 20× dry objective (numerical aperture 0.40) unless otherwise stated. The investigation was concentrated on the beads that moved smoothly under various rates of rotation of the rotor.

The amount of centrifugal force (=load) F on the bead is given by:

$$F = \Delta\rho V r \omega^2 ,$$

where $\Delta\rho$ is the difference in density between the bead and the surrounding medium (0.3 g cm^{-3}), V is the bead volume (12 μm^3), r is the effective radius of centrifugation (4.5–7 cm) and ω is the angular velocity of the rotor. The velocity of bead movement under constant load was determined from the video recordings. The change in position of the bead from frame to frame was measured on the monitor screen (30 cm×20 cm; magnification 2000×) to within less than 0.5 μm using a video microscaler (For-A) (Oiwa *et al.* 1990).

Experiments were also carried out in which the centrifugal forces required to break rigor and Ca^{2+}-induced actin–myosin linkages were determined in the following way. Rigor solution was prepared as the Mg-ATP solution, with the omission of ATP and the addition of hexokinase (500 i.u. ml^{-1}) and D-glucose (2 mmol l^{-1}). The hexokinase–glucose system was used to eliminate ATP remaining in the internodal cell (Oiwa *et al.* 1991). Ca^{2+} solution was prepared by omitting EGTA from, and adding 5 mmol l^{-1} $CaCl_2$ to, Mg-ATP solution. The internodal cell preparations containing either rigor solution or Ca^{2+} solution were observed with a Nikon 10× dry objective (numerical aperture 0.25), and the number of beads attached to actin cables within a given microscopic field (30–50) was counted. The beads were then subjected to centrifugal forces that increased in a stepwise manner over time (see Fig. 7, inset), and the numbers of beads within the same microscopic field were determined from video records at the end of each centrifugation period.

All experiments were performed between June and September 1993 at a room temperatures of 24–26 °C.

Results

Properties of unloaded bead movement along actin cables

We examined the properties of the bead movement along the actin cables when unloaded, i.e. without application of centrifugal forces. The beads were observed to move along the actin cables in one direction with constant velocities of 32–61 μm s^{-1} (mean ± S.D., 46±8.7 μm s^{-1}; N=14). These maximum unloaded velocities (V_{max}) were similar to those of native cytoplasmic streaming and were many times greater than the corresponding movement of beads coated with rabbit skeletal muscle myosin (2.5 μm s^{-1}, Sheetz and Spudich, 1983; 2.0 μm s^{-1}, Oiwa *et al.* 1990). The direction of bead movement was also similar to that of native cytoplasmic streaming, being reversed across the indifferent zone separating two groups of actin cables with different polarities (Kersey *et al.* 1976). The bead movement was inhibited either by the removal of ATP (rigor solution) from the surrounding medium or in the presence of Ca^{2+} (>10^{-6} mol l^{-1}), as has been noted for native cytoplasmic streaming (Williamson, 1975;

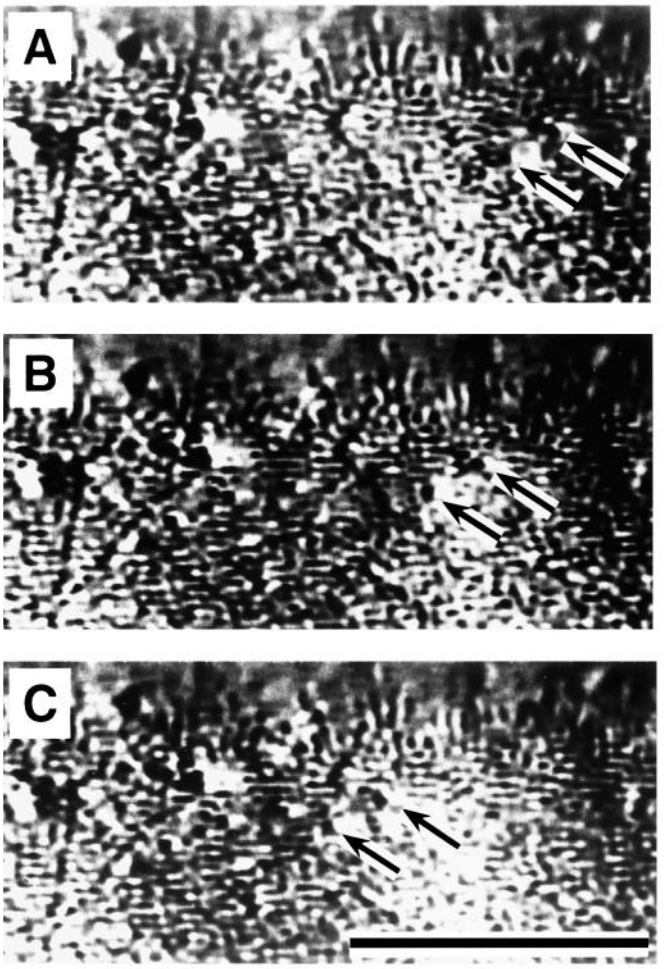

Fig. 1. Selected video frames showing the movement (from right to left) of cytoplasmic myosin-coated beads on actin cables. Arrows indicate the positions of two beads. Frames A, B and C were taken consecutively at intervals of 33.3 ms between frames. Scale bar, 100 μm.

Tominaga *et al.* 1983). These results, together with the occurrence of myosin in algal cell cytoplasm (Kato and Tonomura, 1977), indicate that the rapid bead movement along actin cables is produced by cytoplasmic myosin molecules attached to the bead surface. Fig. 1 shows selected frames from a video recording of the beads moving on actin cables.

Steady-state force–velocity relationships for bead movement under positive loads

Fig. 2 shows a typical result of the application of positive loads (centrifugal forces directed in the opposite direction to the bead movement) on bead movement. The bead moved at a constant velocity under a given positive load, indicating the presence of a definite steady-state relationship between the force (=load) generated by the myosin molecules interacting with the actin cables and the velocity of actin–myosin sliding. The velocity of bead movement decreased with increasing positive load, and the bead eventually stopped moving when the load became equal to the maximum isometric force (P_0)

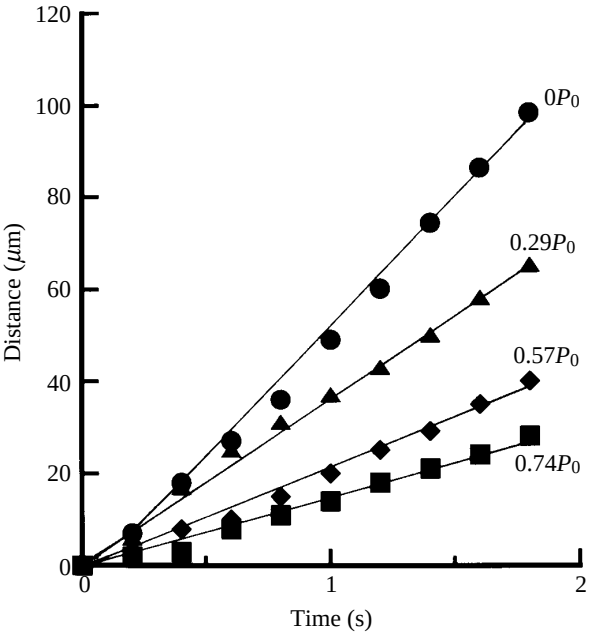

Fig. 2. Constant velocity movements of a cytoplasmic myosin-coated bead on the actin cables under four different positive loads. Regression lines were drawn by the least-squares method. The load (given beside each line) is expressed relative to P_0. The value taken for P_0 was 13 pN, the maximum we measured.

generated by the myosin molecules on the bead. The beads that stopped moving remained in the same position for 5–10 s and then suddenly detached from the actin cables and flowed away in the direction of the applied centrifugal force. The value of P_0 showed considerable variation, ranging from 1.0 to 13 pN (mean ± S.D., 6.2±4.5 pN; N=12).

The steady-state force–velocity relationship of bead movement was determined by applying various constant positive loads and recording the corresponding bead movements. The magnitude of the centrifugal force was either gradually increased to P_0 or randomly altered, with similar results. The difficulty we encountered in the present experiments was that, as the beads moved much faster under every load compared with our previous experiments with rabbit skeletal muscle myosin (Oiwa *et al.* 1990), many beads left the microscopic field before we could determine a value for P_0, i.e. the end point of the force–velocity curve. A typical example of the force–velocity relationship obtained from a bead (P_0=13 pN) is presented in Fig. 3 (filled circles). The force–velocity relationship was nearly straight. The viscous drag force f on the moving bead can be calculated from $f=6\pi\eta rv$, where η is the viscosity of the medium ($0.001\ \mathrm{N\,s\,m^{-2}}$), r is the bead radius (1.4 μm) and v is the bead velocity (in $\mu\mathrm{m\,s^{-1}}$). For v=60 $\mu\mathrm{m\,s^{-1}}$, for example, the drag force is 1.6 pN, amounting to more than 10 % of measured values of P_0. In Fig. 3, the data points corrected for the viscous drag are also shown (open circles); this correction does not alter the shape of the force–velocity curve obtained.

Similar force–velocity relationships were obtained from five

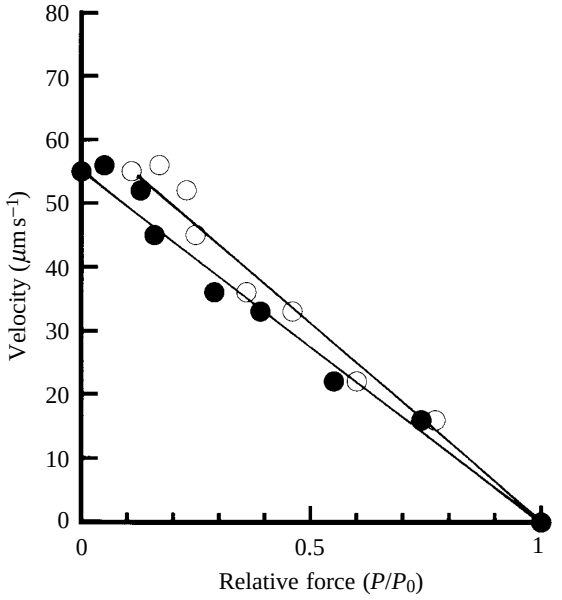

Fig. 3. Typical example of the steady-state force–velocity relationship for bead movement under positive load (filled circles). The data points were obtained by applying loads in a random order. The amount of force (=load) is expressed relative to P_0 (13 pN). Data points corrected for the viscous drag force (open circles) are also shown.

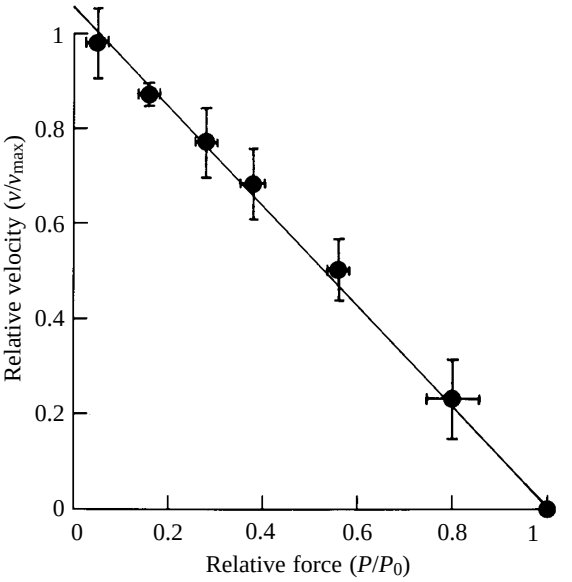

Fig. 4. Averaged steady-state force–velocity relationship for positive load, constructed from six different force–velocity data sets of six beads with large P_0 values (8.6–13 pN). Here and in Fig. 5, data points represent mean values with vertical and horizontal bars indicating standard deviations.

other beads examined, all of which had large P_0 values (8.6–13 pN). Fig. 4 shows the force–velocity curve constructed from these beads. The force–velocity curve cannot be fitted to the Hill hyperbolic equation (Hill, 1938) with reasonable accuracy because of its straight shape. In another six beads, with smaller P_0 values (1.0–2.4 pN), the data points showed a large scatter, especially at higher loads, although the overall force–velocity curve was also nearly straight (Fig. 5).

Steady-state force–velocity relationships for bead movement under negative loads

Since the polarity of the actin cables determining the direction of actin–myosin sliding is reversed across the indifferent zone, we also took the opportunity of applying centrifugal forces in the same direction as the bead movement to serve as negative loads. As with positive loads, the beads moved with a constant velocity under a given negative load. A typical force–velocity relationship for negative loads is shown in Fig. 6. When the negative load was gradually increased from zero, the velocity of bead movement first decreased by 10–30 % and then increased with further increases in the negative load until it suddenly detached from the actin cables. Similar results were obtained from eight other beads examined, although the negative force at which the velocity reached a minimum (0.1–0.7 pN) and that at which the bead detached (0.6–3.6 pN) were variable.

Strength of rigor and Ca^{2+}-induced actin–myosin linkages

In the present study, bead movement was found to be completely inhibited either in the absence of ATP or in the presence of Ca^{2+} (5 mmol l^{-1}), indicating that the inhibition of cytoplasmic streaming that is known to occur either in the absence of ATP or in the presence of Ca^{2+} (Williamson, 1975; Tominaga *et al.* 1983) results from inhibition of actin–myosin sliding. In both conditions, the beads stick firmly to the actin cables owing to the formation of static actin–myosin linkages. We compared the centrifugal forces required to break rigor actin–myosin linkages (induced in the absence of ATP) with those required to break Ca^{2+}-induced actin–myosin linkages.

The number of beads sticking to the actin cables in rigor solution decreased gradually owing to their gradual detachment from the actin cables as the load was increased from 0 to 22 pN (Fig. 7). Similar results were obtained from five other internodal cell preparations containing rigor solution. Since the indifferent zone, across which the actin cable polarity is reversed, was included in the microscopic field, the direction of centrifugal force was either opposite to, or the same as, the direction of bead movement that would have taken place in the ordinary Mg-ATP solution. There was no tendency for the beads to become detached more readily at one side of the indifferent zone than at the other. In contrast, the beads attached to actin cables in Ca^{2+} solution did not detach from actin cables with increasing centrifugal forces up to 22 pN (Fig. 5). These results indicate that rigor actin–myosin linkages can be broken more readily with applied centrifugal forces than can Ca^{2+}-induced actin–myosin linkages. However, the beads attached to the actin cables in Ca^{2+} solution could be detached from the actin cables on removal of Ca^{2+} from the solution, demonstrating the reversibility of the Ca^{2+}-dependent actin–myosin linkages.

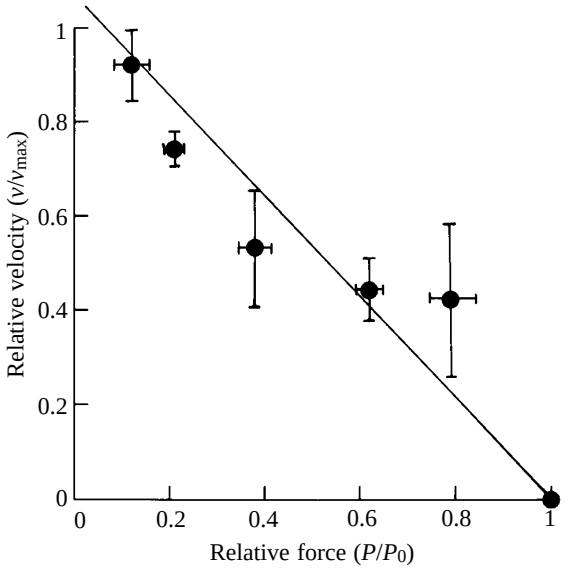

Fig. 5. Averaged steady-state force–velocity relationship for positive load, constructed from six different force–velocity data sets from six beads with small P_0 values (1.0–2.4 pN).

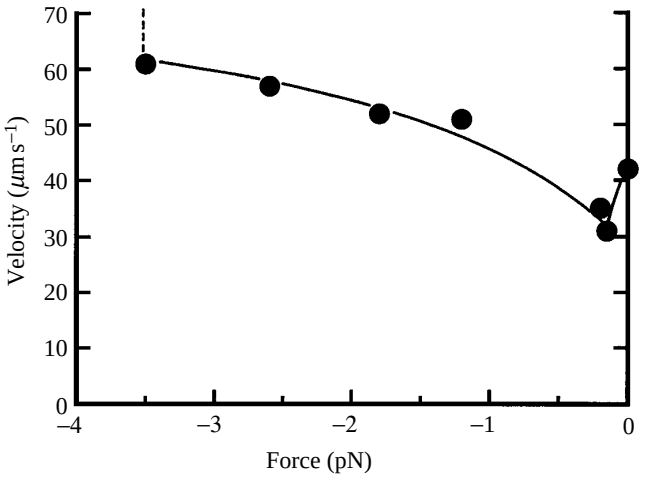

Fig. 6. Steady-state force–velocity relationship for the movement of a bead under negative loads. The force (=load) is expressed in pN. The bead became detached from the actin cables at a negative load of 3.5 pN.

Discussion

Kinetic properties of actin–myosin sliding causing cytoplasmic streaming in algal cells

Using an *in vitro* assay system combined with a centrifuge microscope (Oiwa *et al.* 1990), we have shown that beads coated with cytoplasmic myosin move along actin cables at a constant velocity under a constant external load (Fig. 2). We have determined the steady-state force–velocity relationships under both positive and negative loads (Figs 3–6), thus providing the first information about the kinetic properties of the actin–myosin sliding that causes cytoplasmic streaming in plant cells. We shall first discuss the force–velocity relationships in the positive load region (Fig. 3), as they can be compared directly with known force–velocity relationships for contracting muscle.

The hyperbolic force–velocity curve of contracting muscle is generally characterized using the values V_{max} and a/P_0 (Woledge *et al.* 1985); the former determines its intercept with the velocity axis, while the latter determines its curvature. A large value of a/P_0 is associated with a less prominent curvature of the force–velocity curve and a low efficiency in the conversion of the chemical energy derived from ATP hydrolysis into mechanical work (Woledge, 1968). On this basis, the nearly straight force–velocity curve that we obtained for cytoplasmic myosin sliding on the actin cables (Fig. 3) suggests a low efficiency for the actin–myosin sliding that causes cytoplasmic streaming. Our value for V_{max} is many times larger than that for skeletal muscle, which suggests that the maximum cycling rate of the actin–myosin interaction is many times larger for cytoplasmic myosin sliding on the actin cables than for the same process in muscle. Thus, our results are consistent with the view that ATP-dependent actin–myosin sliding during cytoplasmic streaming has a much higher maximum cycling rate, and a much lower efficiency, than ATP-dependent actin–myosin sliding during muscle contraction.

Unlike skeletal muscles, which contract only occasionally under various external loads, cytoplasmic streaming in algal cells occurs continuously, at velocities similar to our values of V_{max}, suggesting that cytoplasmic myosin always interacts with the actin cables at the maximum cycling rate during cytoplasmic streaming. There is evidence that cytoplasmic myosin molecules are attached to amorphous cytoplasmic organelles, and that it is the movement of the organelles, caused by actin–myosin sliding, that produces streaming of the surrounding cytoplasm (Williamson, 1975; Shimmen and

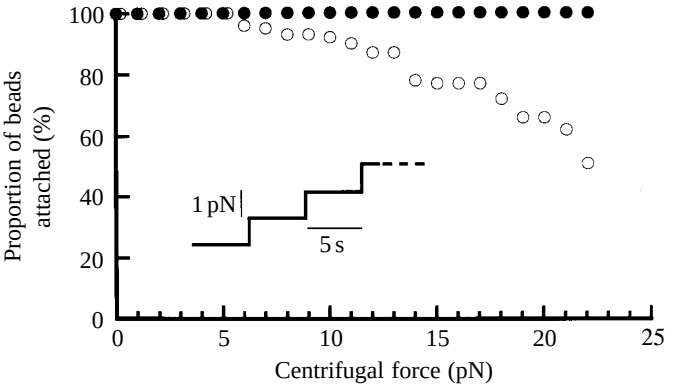

Fig. 7. Effect of centrifugal forces on the proportion of beads attached to actin cables in rigor solution (open circles) and in Ca^{2+} solution (filled circles). The initial number of beads was 110 in rigor solution and 95 in Ca^{2+} solution. Note that the proportion of beads attached to actin cables in rigor solution was gradually reduced to 50 % with increasing load (from 0 to 22 pN), while the beads attached to actin cables in Ca^{2+} solution did not become detached. The inset shows that centrifugal forces were increased every 5 s in 1 pN steps.

Tazawa, 1982). It seems possible that the internal resistance on the myosin molecules attached to the cytoplasmic organelles in cytoplasmic streaming is comparable to the viscous drag on the myosin molecules attached to the beads in the present assay system.

As the negative load applied was gradually increased, the velocity of bead movement was first reduced and then increased (Fig. 6). An analogous effect of negative load, i.e. a reduction in velocity of bead movement, has been observed for rabbit myosin-coated beads moving along actin cables (Oiwa *et al.* 1990) and also for sperm axonemes sliding on a kinesin-coated glass surface (Hall *et al.* 1993). At present, we can offer no explanations for this phenomenon.

Comparison of the present results with other work

The maximum isometric force P_0 generated by the myosin molecules on the bead ranged from 1 to 13 pN. The most straightforward interpretation for this range would be that a single myosin molecule generates a P_0 of 1 pN and that 1–13 myosin molecules are involved in the bead movement. This interpretation may contradict recent reports showing, using *in vitro* motility assay techniques, that a single myosin molecule can generate a force of 1–7 pN (Finer *et al.* 1994) or 5–6 pN (Ishijima *et al.* 1994). However, the experimental conditions used in these studies were completely different from those reported here; they measured peak amplitudes of transient force spikes generated by myosin molecule(s), while in the present experiments the myosin molecule(s) on the bead should continuously generate a force, equal to the applied centrifugal force, to move the bead over many micrometres. Hence, we measured time-averaged forces generated by the myosin molecules on the bead. In addition, the amplitude measured from force spikes is dependent on the relative orientation between actin and myosin (Ishijima *et al.* 1994). The myosin molecules on the bead are likely to be randomly oriented both in the present study and in the experiments of Finer *et al.* (1994). Hence a value of 1 pN for P_0 may not be contradictory with values from *in vitro* assays.

Using techniques identical with those in the present study, Oiwa *et al.* (1990) determined the force–velocity curves for sliding between rabbit skeletal muscle myosin and the actin cables. The curves that they found were hyperbolic in the low force range and nonhyperbolic for higher forces, and this was more pronounced with decreasing P_0. We suggest the following, tentative, explanation for the dependence of the shape of the force–velocity curve on P_0 (S. Sugiura and H. Sugi, unpublished results). According to the Huxley contraction model (Huxley, 1957), muscle contraction results from alternate formation and breakage of actin–myosin linkages. If p is defined as the proportion of time for which a myosin head is detached from actin within each cycle of actin–myosin interaction, the probability that all myosin heads are detached from actin is $P_{off}=p^n$ ($0<p<1$), where n is the number of myosin heads interacting with actin. The value of P_{off} becomes substantial even for small values of n, especially if the value of p is large. When all myosin heads are detached from actin cables, the bead will be pulled back by centrifugal forces, resulting in a back-and-forth bead movement. Since p increases with decreasing external load (Huxley, 1957), this effect will be most marked for the low force range, and this may cause a considerable reduction in the measured values for the actin–myosin sliding velocity for these small forces; that is, a less pronounced hyperbolic part of the force–velocity curve in the low force range.

Hence, use of the concept of P_{off} can qualitatively account for the dependence of force–velocity curves on P_0 (Oiwa *et al.* 1990). In the present work, almost straight force–velocity curves were observed, irrespective of whether P_0 was large or small, indicating that P_{off} is not large even for the small number of cytoplasmic myosin molecules involved. This may be taken to imply that the value of p, i.e. the proportion of time for which a cytoplasmic myosin head is detached from actin within each cycle of interaction, is also small. As the number of cytoplasmic myosin molecules attached to each organelle causing cytoplasmic streaming is expected to be small, this very small value for p may be essential in order to prevent the organelle from becoming detached from the actin cables. In relation to this, it is of interest that p has been demonstrated to be very small for another motor protein, kinesin, which transports cellular components (Howard *et al.*, 1989; Block *et al.* 1990). Recently, Svoboda and Block (1994) analyzed the ATP-dependent motion of kinesin-coated latex beads, using the optical trapping technique, and constructed a straight force–velocity curve analogous to that presented here. In their experiments, however, the bead movement consisted of a series of minute transient motions against a force gradient, and average velocities were plotted against average forces; these transient motions could be influenced by strain-dependent passive elastic components. The steady-state force–velocity curves obtained in the present study were constructed from constant-velocity bead movements over many micrometres under constant centrifugal forces, so that the length of any passive elastic components was kept constant. It would be of interest to use the optical trapping technique to examine the behaviour of beads coated with cytoplasmic myosin.

Effect of Ca^{2+} on cytoplasmic streaming

It is known that, when an algal internodal cell generates an action potential associated with influx of external Ca^{2+} into the cell (Shimmen, 1992), cytoplasmic streaming stops as a result of an increase in cytoplasmic Ca^{2+} concentration (Williamson and Ashley, 1982). Cytoplasmic streaming in internodal cells, made permeable with a Ca^{2+}-free EGTA solution, is reversibly inhibited by Ca^{2+} (Tominaga *et al.* 1983). Myosin heavy chains responsible for cytoplasmic streaming have recently been isolated from the algal internodal cells (K. Yamamoto, personal communication) and the lily pollen tube (T. Shimmen and E. Yokota, personal communication). Their ATPase is activated with actin, and F-actin sliding on a glass surface coated with pollen tube myosin is reversibly inhibited by Ca^{2+}.

In the present study, the beads were found to attach firmly to actin cables in the presence of Ca^{2+}, demonstrating that the

Ca^{2+}-induced inhibition of cytoplasmic streaming is due to the formation of static actin–myosin linkages. Application of centrifugal forces to the beads attached to actin cables showed that rigor actin–myosin linkages could be broken more readily than Ca^{2+}-induced actin–myosin linkages (Fig. 7). This result suggests that Ca^{2+}-induced actin–myosin linkages are much stronger than, and therefore quite different from, rigor linkages. More experimental work is obviously needed to clarify the properties of cytoplasmic myosin, which are different from those of muscle myosin in many respects.

References

Block, S. M., Goldstein, L. S. B. and Schnapp, B. J. (1990). Bead movement by single kinesin molecules studied with optical tweezers. *Nature* **348**, 348–352.

Finer, J. T., Simmons, R. M. and Spudich, J. A. (1994). Single myosin molecule mechanics: piconewton forces and nanometre steps. *Nature* **368**, 113–119.

Hall, K., Cole, D. G., Yeh, Y., Scholey, J. M. and Baskin, R. J. (1993). Force–velocity relationships in kinesin-driven motility. *Nature* **364**, 457–459.

Hill, A. V. (1938). The heat of shortening and the dynamic constants of muscle. *Proc. R. Soc. B* **126**, 136–195.

Howard, J., Hudspeth, A. J. and Vale, R. D. (1989). Movement of microtubules by single kinesin molecules. *Nature* **342**, 154–158.

Huxley, A. F. (1957). Muscle structure and theories of contraction. *Prog. Biophys. biophys. Chem.* **7**, 225–318.

Ishijima, A., Harada, Y., Kojima, H., Funatsu, T., Higuchi, H. and Yanagida, T. (1994). Single-molecule analysis of the actomyosin motor using nano-manipulation. *Biochem. biophys. Res. Commun.* **199**, 1057–1063.

Kamitsubo, E., Ohasi, Y. and Kikuyama, M. (1989). Cytoplasmic streaming in internodal cells of *Nitella* under centrifugal acceleration: A study done with a newly constructed centrifuge microscope. *Protoplasma* **152**, 148–155.

Kamiya, N. and Kuroda, K. (1956). Velocity distribution of the protoplasmic streaming in *Nitella* cells. *Bot. Mag., Tokyo* **69**, 544–554.

Kato, T. and Tonomura, Y. (1977). Identification of myosin in *Nitella flexilis*. *J. Biochem., Tokyo* **82**, 777–782.

Kersey, Y. M., Hepler, R. K., Palevitz, B. A. and Wessels, N. K. (1976). Polarity of actin filaments in Characean algae. *Proc. natn. Acad. Sci. U.S.A.* **73**, 165–167.

Kersey, Y. M. and Wessels, N. K. (1976). Localization of actin filaments in internodal cells of Characean algae. *J. Cell Biol.* **68**, 264–275.

Nagai, R. and Rebhum, L. (1966). Cytoplasmic microfilaments in streaming *Nitella* cells. *J. Ultrastruct. Res.* **14**, 571–589.

Oiwa, K., Chaen, S., Kamaitsubo, E., Shimmen, T. and Sugi, H. (1990). Steady-state force–velocity relation in the ATP-dependent sliding movement of myosin-coated beads on actin cables *in vitro* studied using a centrifuge microscope. *Proc. natn. Acad. Sci. U.S.A.* **87**, 7893–7897.

Oiwa, K., Chaen, S. and Sugi, H. (1991). Measurement of work done by ATP-induced sliding between rabbit muscle myosin and algal cell actin cables *in vitro*. *J. Physiol., Lond.* **437**, 751–763.

Sheetz, M. P. and Spudich, J. A. (1983). Movement of myosin-coated fluorescent beads on actin cables *in vitro*. *Nature* **303**, 31–35.

Shimmen, T. (1992). Mechanism of cytoplasmic streaming and amoeboid movement. In *Muscle Contraction and Cell Motility, Molecular and Cellular Aspects, Advances in Comparative and Environmental Physiology*, vol. 12 (ed. H. Sugi), pp. 172–205. Berlin, Heidelberg: Springer Verlag.

Shimmen, T. and Tazawa, M. (1982). Reconstitution of cytoplasmic streaming in Characeae. *Protoplasma* **113**, 127–131.

Shimmen, T. and Yano, M. (1984). Active sliding movement of latex beads coated with skeletal muscle myosin on *Chara* actin bundles. *Protoplasma* **121**, 132–137.

Svoboda, K. and Block, S. M. (1994). Force and velocity measured for single kinesin molecules. *Cell* **77**, 773–784.

Tazawa, M., Kikuyama, M. and Shimmen, T. (1976). Electric characteristics and cytoplasmic streaming of Characeae cells lacking tonoplast. *Cell Struct. Funct.* **1**, 165–176.

Tominaga, Y., Shimmen, T. and Tazawa, M. (1983). Control of cytoplasmic streaming by extracellular Ca^{2+} in permealized *Nitella* cells. *Protoplasma* **116**, 75–77.

Williamson, R. E. (1975). Cytoplasmic streaming in *Chara*: A cell model activated by ATP and inhibited by cytochalasin B. *J. Cell Sci.* **17**, 655–668.

Williamson, R. E. and Ashley, C. C. (1982). Free Ca^{2+} and cytoplasmic streaming in the alga *Chara*. *Nature* **296**, 647–651.

Woledge, R. C. (1968). The energitics of tortoise muscle. *J. Physiol., Lond.* **197**, 685–707.

Woledge, R. C., Curtin, N. A. and Homsher, E. (1985). Mechanics of contraction. In *Energetic Aspects of Muscle Contraction, Monographs of the Physiological Society*, no. 41, pp. 27–117. London, New York: Academic Press.